Available online at www.sciencedirect.com

ScienceDirect

Energy Procedia 4 (2011) 4937–4944

Energy Procedia

www.elsevier.com/locate/procedia

GHGT-10

CO_2-porewater-rock reactions - Large-scale column experiment (Big Rig II)

Keith Bateman, Christopher Rochelle, Alicja Lacinska, Doris Wagner

British Geological Survey, Kingsley Dunham Centre, Keyworth, Nottingham, NG12 5GG, UK

Abstract

This study focused on the reactions between carbon dioxide (CO_2), porewater and host rock during geological CO_2 storage in deep reservoirs. The aim of this work was to provide a well-constrained laboratory experiment reacting known quantities of minerals with CO_2-rich fluids, to simulate situations where CO_2 is being injected into lithologies deep underground.
The experiment was undertaken using a Ti-column, 100 cm long, held within a large pressure vessel. The column was packed with a simplified mineral assemblage. The reactant fluid was equilibrated with CO_2 at a temperature of 130ºC and a pressure of 300 bar, before being pumped into the column held under the same conditions. Fluid was passed along the column at a constant flow rate for approximately 3.5 months. Fluids collected from the outlet end of the column were analysed to provide data on the fate of the dissolved species. On completion of the experiment, the column was then examined for mineralogical changes. The experimental results can be used as a test case for predictive geochemical computer modelling. Such models will help improve our ability to predict the long-term fate of CO_2 stored underground.

Keywords :- CO_2, laboratory experiment, geochemistry, porewater

1. Introduction

During underground carbon dioxide (CO_2) storage operations in deep reservoirs, the CO_2 can be trapped in three ways; as 'free' CO_2, most likely as a supercritical phase (physical trapping); dissolved in formation water (hydrodynamic trapping); precipitated in carbonate phases such as calcite (mineral trapping). During the early stages of storage, 'physical trapping' is likely to be the most important trapping mechanism. However, over time, hydrodynamic trapping and eventually mineral trapping will make significant contributions to the long-term containment of CO_2. This study focuses on the reactions between CO_2, porewater and host rock.

Computer models are routinely used to predict the long-term fate of CO_2 stored underground. However, it is important to have confidence in the predictive capability of these models. This can be achieved through validation of the models with example 'test cases'. The work described in this paper was aimed at providing a well-constrained, laboratory experiment reacting known quantities of minerals with CO_2-rich fluids, the results of which could then be used as one such 'test case'. A limitation of such laboratory experiments are the timescales over which they run, and therefore any models will need to be validated against a number of such experiments representing the evolution of an underground CO_2 store, as well a well characterised natural systems.

doi:10.1016/j.egypro.2011.02.463

Within an underground CO_2 storage operation there will be a region of free CO_2 (e.g. the CO_2 'bubble') overlying original formation porewater. The CO_2 will dissolve into the formation water at a rate controlled by factors such as: the rate of CO_2 injection, the rate of CO_2 dissolution into the porewater, the chemistry of the porewater, the surface area available for reaction, and the rate of diffusion of the CO_2 into the porewater away from the porewater-CO_2 interface. Therefore, in different parts of the formation there will exist porewaters with a range of dissolved CO_2 concentrations. Within an experimental programme, it is not possible to simulate all possible dissolved CO_2 concentrations, so the 'CO_2-saturated' case where maximum CO_2 is dissolved into the porewater was chosen, since it is anticipated that maximising aqueous CO_2 concentrations will maximise the degree of fluid-rock reaction and provide a 'limiting case' for study. The experiment was conducted within The Hydrothermal Laboratory of the British Geological Survey, Keyworth, UK.

2. Experimental setup

2.1. Equipment

Prior to performing the experiments, it was necessary to design and construct equipment that would perform well. Although dry supercritical CO_2 is relatively inert, in the presence of water or saline solution it is much more reactive. Previous studies [1] have shown that steel will corrode and standard 'O-ring' seals will blister and fail. To minimise both corrosion and experimental failure, exposed surfaces were chosen to be as inert as practicable. Therefore, the wetted parts of the steel vessels (stainless steel type 316) were generally lined with titanium, the high-pressure tubing was made of 316 grade stainless steel, and the column was titanium with stainless steel end-caps. The pressurized fluid sampling containers were constructed entirely from titanium.

A simplified schematic of the complete experimental system is shown in Figure 1. Essentially, the equipment consists of a titanium column 100 cm long, with an internal diameter of 3.6 cm containing the packed reacting mineral assemblage. This titanium column is held within a large heated pressure vessel (aka the 'Big Rig'), with the confining pressure of the vessel being maintained by a syringe pump. A purpose built (Baskerville Reactors and Autoclaves Ltd), 3 litre capacity, conditioning vessel was used, to pre-equilibrate the reactant fluid with CO_2 under the experimental conditions. Syringe pumps were used to raise the pressure to the operating pressure. The reactant fluid was equilibrated with CO_2 at the experimental temperature and pressure, before being displaced by the pressurising CO_2. The CO_2 pressure was maintained using a syringe pump. A third syringe pump controlled fluid flow out of the column. Samples of the reactant fluid were collected using a 30 ml capacity, titanium floating piston pressure sampler.

2.2. Starting Materials

The fluids and mineral assemblage used in the experiment were based upon simplified versions of those in the Saline Aquifer CO_2 Storage (SACS) project [2]. The chemical composition of the fluid prior to equilibration with CO_2 was $[Na^+]$ = 0.5 Mol.dm^{-3}, $[K^+]$ = 1.35 x 10-10 Mol.dm^{-3}, $[Ca^{2+}]$ = 1.2×10-3 Mol.dm^{-3}, $[Cl^-]$ = 0.502 Mol.dm^{-3}, $[HCO_3^-]$ = 1.59 x 10-4 Mol.dm^{-3}. The mineral assemblage comprised rounded and sub-rounded grains of quartz, angular and blocky grains of labradorite, K-feldspar, platy mica and euhedral to subhedral, calcite that was typically fractured along the cleavage. No evidence for dissolution or precipitation was seen in the starting material. In terms of abundances, it comprised; quartz (70 wt%), labradorite (20 wt%), calcite (5 wt%), and muscovite (5 wt%). Most solids were prepared from individual mineral specimens that were crushed and sieved to 125-250 μm. The quartz was obtained as quartz sand (Sigma-Aldrich).

The column was packed with the simplified mineral assemblage the initial total weight of the mineral mixture was 1298 g. The initial porosity of the column was determined to be 44.1%. The reactant fluid was equilibrated with CO_2 at a temperature of 130ºC and a pressure of 300 bar, before being pumped into the column held under the same conditions. Compared to previous work [3] a relativity high temperature of 130°C was selected. Use of an elevated temperature will increase the rates of reaction and thus allow more reaction to occur within the limited timescale available for laboratory experiments, this should also result in chemical and mineralogical changes being observable with the currently available analytical techniques. The selection of 130°C is still within the likely upper range of temperatures for a potential CO_2 storage site. Fluid was passed along the column at a constant flow rate of

5 cm^3h^{-1} for approximately 3.5 months. On completion of the experiment, the column was recovered from the pressure vessel, sectioned into many pieces, and examined for mineralogical changes. Fluids collected from the outlet end of the column were analysed to provide data on the fate of the dissolved species.

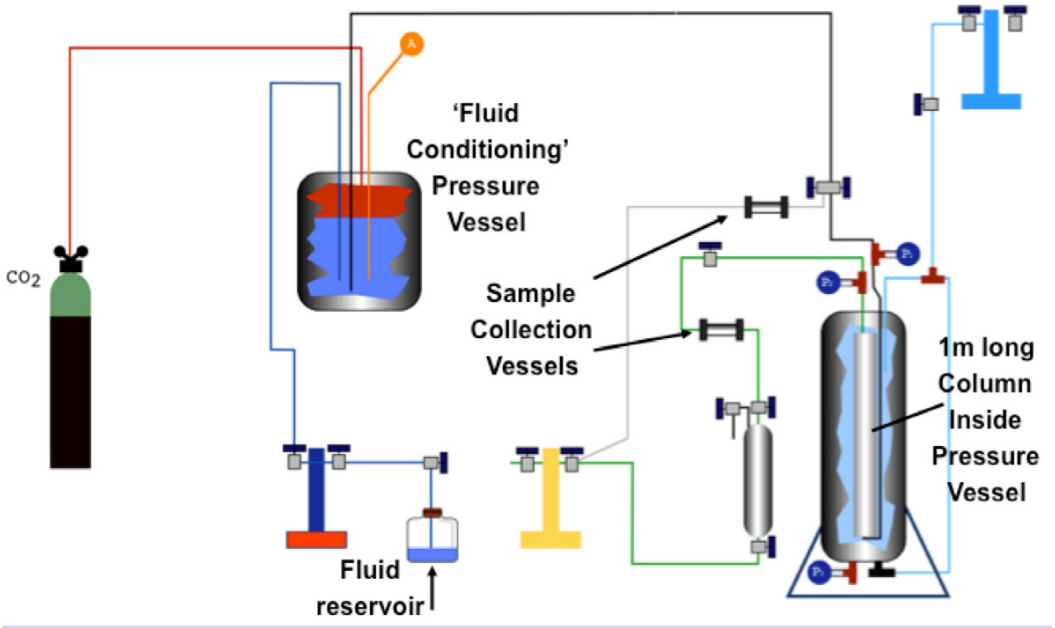

Figure 1 Schematic of the experimental setup.

2.3. Analytical Methods

Samples of the reactant fluid were collected using a titanium floating piston pressure sampler. The reacted fluid was then rapidly depressurised before being prepared for chemical analysis. Samples of the unreacted and reacted fluids were split into several sub-samples. A sub-sample of 1 ml was taken for immediate analysis of pH. Measurements of pH were made using a pH meter calibrated using Whatman® NBS traceable buffers at pH 4, 7, and 10, all measurements were performed at 20°C, and atmospheric pressure. Another sub-sample of 2 ml was taken for immediate analysis of bicarbonate concentration by titration.

Another sub-sample was taken using a polythene syringe and filtered using a 0.2 µm 'Anotop'® nylon syringe filter. A 10 ml aliquot of this sample was pipetted into a polystyrene tube and acidified with 0.1 ml of concentrated 'ARISTAR'® nitric acid. This sample was analysed subsequently for major and trace cations by inductively coupled plasma - optical emission spectroscopy (ICP-OES). A further aliquot of the filtered sample (approximately 4 ml) was also taken and placed in a polyethylene tube for analysis of anions by ion chromatography (IC). All fluid samples were stored in a fridge (at about 5°C) prior to analysis.

Solids for analysis were prepared as grain mounts and coated with a thin layer of carbon, for examination by Scanning Electron Microscope (SEM). Analyses were performed using a variable pressure (VP) LEO 435 digital scanning electron microscope. The SEM instrument was equipped with an Everhart-Thornley type detector used for secondary electron imaging and a KE Developments four-quadrant (4 diode-type) solid-state detector for backscattered electron imaging (BSEM). Mineral compositions were obtained using an Oxford Instruments INCA energy-dispersive X-ray microanalysis system (EDXA). Quantitative X-ray diffraction (XRD) analysis was performed using a PANalytical X'Pert Pro series diffractometer.

3. Results

3.1. Fluid Chemistry

Table 1 shows the fluid chemistry data, the pH (at 20°C, 1 bar) of the initial un-equilibrated fluid was = 7.1. After equilibration with CO_2 at the experimental conditions, the measured pH (at 20°C, 1 bar) was ≈ 6.5. During the experiment, the pH (at 20°C, 1 bar) of the sampled reacted fluids remained constant ≈ 6.1±0.1. Using a specially developed cell it was also possible to obtain a measurement of pH under in-situ conditions (temperature and pressure) which gave an in-situ pH (at 130°C, 300 bar) = 4.7.

The bicarbonate concentrations of the initial unreacted, CO_2-equilibrated fluid was ≈ $2x10^{-3}$ mol.l^{-1} and this increased in the initial reacted fluids to approximately $2.6x10^{-2}$ mol.l^{-1}, during the rest of the experiment the levels of bicarbonate remain similar throughout.

Table 1 Fluid chemical data

Sample No	Time (hours)	pH (1 bar, 20°C)	pH (300 bar)	HCO_3^-	Ca^{2+}	Mg^{2+}	Na^+	K^+	Si	Ba	Sr
1235/Start	-	7.10			1.08E-3	<1.65E-5	4.84E-1	<5.12E-4	<1.07E-4	<5.83E-7	<2.28E-6
1235/CO_2	-	6.50	3.54	2.07E-3	9.70E-4	<8.23E-6	4.41E-1	<2.56E-4	<5.34E-5	<2.91E-7	<1.14E-6
1235/1	174	6.19		2.63E-2	1.13E-2	6.85E-4	4.38E-1	1.71E-3	5.85E-3	8.86E-6	4.18E-6
1235/2	366	6.28		2.67E-2	1.17E-2	8.32E-4	4.50E-1	1.17E-3	3.12E-3	8.78E-6	4.97E-6
1235/3	448	6.16		2.72E-2	1.19E-2	1.27E-3	4.49E-1	<5.12E-4	3.35E-3	8.01E-6	5.19E-6
1235/4	636	6.17		2.55E-2	1.27E-2	6.50E-4	4.27E-1	<5.12E-4	2.56E-3	5.52E-6	4.13E-6
1235/5	759	6.04		2.56E-2	1.24E-2	5.93E-4	4.24E-1	<5.12E-4	2.42E-3	4.51E-6	4.51E-6
1235/6	971	6.04		2.38E-2	1.20E-2	5.64E-4	4.19E-1	<5.12E-4	2.36E-3	6.67E-6	5.16E-6
1235/7	1287	6.05		2.39E-2	1.16E-2	4.93E-4	4.09E-1	<5.12E-4	2.23E-3	1.02E-5	4.83E-6
1235/8	1428	6.11		2.37E-2	1.16E-2	4.92E-4	4.13E-1	<5.12E-4	2.22E-3	3.18E-6	4.21E-6
1235/9	1574	6.18		2.49E-2	1.15E-2	4.85E-4	4.17E-1	<5.12E-4	2.18E-3	4.51E-6	4.36E-6
1235/10	1897	6.15		2.33E-2	1.13E-2	5.23E-4	4.44E-1	<5.12E-4	2.25E-3	3.71E-6	5.62E-6
1235/11	2378	6.11	4.65	2.28E-2	1.18E-2	4.94E-4	4.47E-1	<5.12E-4	2.33E-3	5.74E-6	5.10E-6
1235/12	2541	6.04	4.65	2.29E-2	1.14E-2	4.52E-4	4.60E-1	<5.12E-4	2.20E-3	7.44E-6	4.71E-6

Sample No	Time (hours)	Mn	Total Fe	Al	Ni	Zn	Cr	Cl	SO_4
1235/Start	-	<1.46E-6	<7.16E-6	<1.48E-5	<3.41E-6	<3.06E-6	<1.54E-6	5.12E-1	1.36E-4
1235/CO_2	-	<7.28E-7	<3.58E-6	<7.41E-6	<1.70E-6	<1.53E-6	<7.69E-7	n.d.	9.91E-4
1235/1	174	1.64E-6	2.96E-4	<1.48E-5	1.97E-5	4.75E-6	3.32E-6	4.98E-1	<1.04E-4
1235/2	366	1.75E-6	3.76E-4	<1.48E-5	6.18E-5	1.47E-5	<1.54E-6	4.83E-1	1.62E-4
1235/3	448	1.90E-6	3.55E-4	<1.48E-5	5.56E-5	3.84E-6	3.22E-6	4.80E-1	2.25E-4
1235/4	636	1.92E-6	3.67E-4	<1.48E-5	4.77E-5	<3.06E-6	3.03E-6	4.57E-1	<1.04E-4
1235/5	759	1.86E-6	3.58E-4	<1.48E-5	3.44E-5	<3.06E-6	4.16E-6	4.74E-1	<1.04E-4
1235/6	971	1.80E-6	3.32E-4	<1.48E-5	3.03E-5	<3.06E-6	2.42E-6	4.52E-1	<1.04E-4
1235/7	1287	<1.46E-6	2.71E-4	<1.48E-5	3.76E-5	<3.06E-6	<1.54E-6	4.39E-1	<1.04E-4
1235/8	1428	<1.46E-6	2.98E-4	<1.48E-5	4.52E-5	<3.06E-6	<1.54E-6	4.46E-1	<1.04E-4
1235/9	1574	1.80E-6	3.27E-4	<1.48E-5	5.71E-5	<3.06E-6	3.45E-6	4.59E-1	1.22E-4
1235/10	1897	1.53E-6	3.05E-4	<1.48E-5	4.75E-5	<3.06E-6	3.66E-6	4.80E-1	<1.04E-4
1235/11	2378	1.85E-6	2.71E-4	<1.48E-5	4.26E-5	<3.06E-6	1.96E-6	4.81E-1	<1.04E-4
1235/12	2541	<1.46E-6	2.43E-4	<1.48E-5	3.85E-5	3.08E-6	<1.54E-6	4.95E-1	<1.04E-4

1235/Start – Unreacted fluid before equilibration with CO_2

1235/ CO – Unreacted fluid after equilibration with CO_2

For most of the experiment, there was little change in the concentration of sodium and chloride from the relatively high starting values. Calcium shows a large increase in concentration in the initial reacted fluids (from ≈ $1x10^{-2}$ mol.l^{-1}, to ≈ $2.3x10^{-2}$ mol.l^{-1}) but then shows little variation in concentration during the remainder of the experiment. This increase in concentration is likely to be the result of dissolution of the calcite present in the mineral assemblage. Magnesium shows a similar trend to that of calcium, from ≈ $4x10^{-6}$ mol.l^{-1} in the unreacted

fluid to ≈ $4x10^{-4}$ mol.l^{-1} later in the experiment. Ba and Sr show similar behaviour.

Iron and manganese concentrations, both show real increases in concentration from that of the unreacted fluid but there is no obvious trend in the data. It is thought that one possible source for these elements in the reacted fluids, is the stainless steel used in parts of the experimental equipment. Further evidence for the corrosion of the stainless steel is seen in the increases in the Ni, Zn, and Cr concentrations observed in the reacted fluids. Aluminium and potassium concentrations, throughout the experiment, were close to or below that of the ICP detection limit.

The results for silica show a slightly different behaviour, in that the concentration rose sharply in the first 200 hours of reaction from a starting value below the detection limit of the ICP to ≈ $6x10^{-3}$ mol.l^{-1}. There then follows a decrease in concentration over the next 600 hours of reaction to ≈ $2.3x10^{-3}$ mol.l^{-1}. The concentration of silica then remained close to this value for the remainder of the experiment. The initial rapid increases in silica concentration may have been the result of preferential dissolution of fines produced during the sample preparation. The later reduced levels of silica may therefore be more representative of the behaviour of the mineral assemblage

4. Mineralogical observations

On completion of the experiment, the fluid in the column was replaced (at the experimental pressure) with propan-2-ol, this was performed in order to 'flush out' reacted fluids and prevent the formation of salts, which would hinder the mineralogical observations. The column was then divided into approximately 2.5 cm intervals, which were stored separately. Subsamples were selected from known intervals from the column, these subsamples were then air-dried for 48 hours. Specimens were than prepared as grain mounts and subsequently coated with a thin layer of carbon.

4.1. Starting Material

Prior to analysis of the reacted intervals, a sample of the starting material was examined. The starting material comprises a synthetic mineral composition. Most of the analysed sample of the starting material is composed of rounded and sub-rounded grains of quartz (locally etched due to sample preparation), angular and blocky grains of labradorite, K-feldspar, platy mica and euhedral to subhedral calcite which is typically fractured along the cleavage. Mineral grain size ranges from about 100 μm to about 500 μm. No evidence for dissolution or precipitation was seen in the starting material.

4.2. Behaviour of $CaCO_3$ (calcite + authigenic phases associated with calcite)

Calcite is a very reactive component of the mineral assemblage used in the experiment. Changes in calcite morphology are observed almost immediately at the beginning of the experimental column (0-3 cm, Figure 2). Deep dissolution pits (up to 10 μm in size) are developed on the crystal surfaces. The crystals decrease in size from about 300 μm in diameter in the starting material to less than 100 μm in the first subsample, and decreases further to less than 50 μm in the 8-10.5 cm subsample. Calcite dissolution takes place along the crystal edges and cleavage as well as on the crystal faces (Figure 2). This results in a change in morphology to that of sub rounded, subhedral to anhedral grains. The gradual dissolution, along with a decrease in size, leads to complete removal of calcite in the subsample from the interval 10.5-13 cm. From this point until the subsample taken at the 28-30.5 cm interval, calcite is absent. The gradual disappearance of the calcite is confirmed by XRD analysis.

In the subsample 28-30.5 cm, original calcite is present, resembling the morphology of the calcite from starting material, although some evidence of etching is still observed. This is seen on the crystal surfaces and crystal edges. In the interval, 70.5-75.5 cm, calcite remains mostly fresh with minor evidence of dissolution. In hand specimen, many <0.5 mm aggregates occurred (whereas all other subsamples were disaggregated to individual sand particles). SEM observations revealed that those aggregates comprised of sand particles, partially cemented together with anhedral, intergranular cement (Figure 3). XRD analysis also showed the appearance of an additional calcite phase that differs slightly from the original composition. This is indicated by a change in crystal lattice spacing from 3.03Å of the original calcite to 3.01Å. At the end of the experimental column, there is no evidence for cementation, calcite remains fresh and resembles the calcite from the starting material with minor corrosion.

4.3. Behaviour of plagioclase (labradorite).

In the starting material, labradorite occurs as clean, blocky crystals with sharp crystal edges. After it has reacted with the injected fluid, it develops many characteristic dissolution features. Between the inlet and up to ≈ 18 cm from the inlet, labradorite is significantly corroded. Labradorite dissolution occurs preferentially along the crystal boundaries, along the cleavage (parallel etching edges) and along defect-distorted sites as well as on the crystal faces as deep etching pits (up to 20 µm long). The preferential dissolution could be due to the compositional variations of the starting material. Further, down the experimental column (from 18 cm onwards) labradorite remains mostly fresh with minor corrosion.

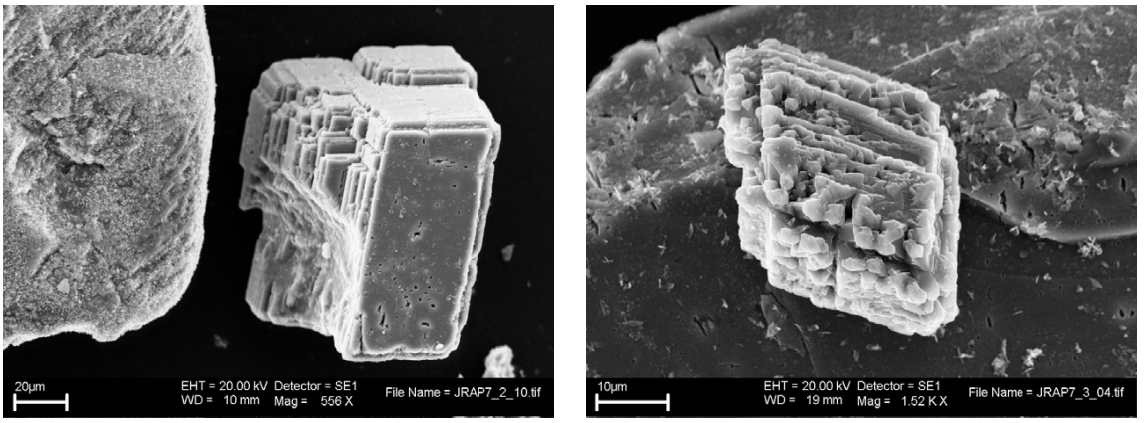

a b

Figure 2 Secondary electron photomicrographs. (a) quartz grain (left) and calcite (right). Calcite shows evidences for dissolution on crystal faces and edges (subsample 0-3 cm). (b) crystal of calcite on top of locally etched labradorite. Note the extensive dissolution of calcite along crystal boundaries (subsample 5.5-8 cm).

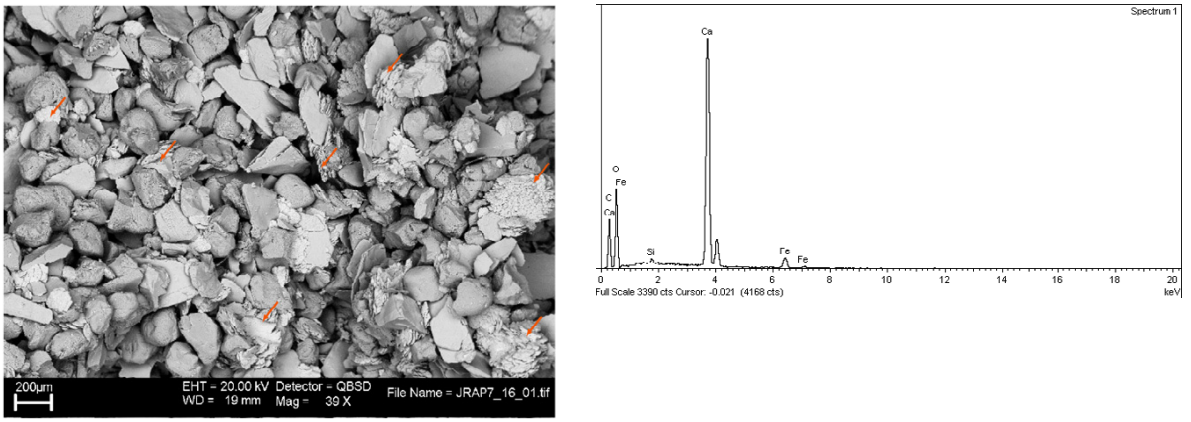

a b

Figure 3 Backscattered electron photomicrographs. (a) showing intergranular, anhedral cement (red arrows) which bonds sand grains together (subsample 75.5-78 cm). (b) EDXA spectrum of the cement shown in (a)

4.4. Behaviour of other minerals.

Other mineral phases, which constitute the remaining components of the starting material, do not show any significant changes after reaction with the injected fluid. Neither the morphology nor the composition show significant changes. Quartz shows some evidence for corrosion on the grain surface (Figure 2). Muscovite does not show any evidence of dissolution throughout the whole length of the experimental column.

4.5. Precipitates.

As a result of reaction between the injected solution and the dissolving minerals, precipitation of new mineral phases has occurred. Secondary mineral phases are developed in the first interval of the experimental column. In the subsample 0-3 cm, most of mineral grains are covered with a thin <1 μm coating (Figure 4), which comprises of two types of distinctly different crystals:

a) Mostly euhedral to subhedral, elongated, locally platy crystals, of less than 2 μm in size (Figure 4b). The crystals were seen to form radiating aggregates. SEM-EDXA analysis revealed that they were composed of an Al-rich phase. Due to their small crystal size and possible interference by underlying quartz grains, the SEM-EDXA analysis on its own does not give a definite composition. XRD analysis confirmed the presence < 0.5% of boehmite (γ-AlO(OH)).

b) Hexagonal, platy crystals (occasionally distorted and possibly twinned) of < 5 μm in diameter (Figure 4b). They were less abundant and unevenly scattered in between the crystals described in (a). The SEM-EDXA analysis also suggested an Al-rich phase.

The proportion of Al-rich crystals gradually decreases further down the column and is no longer observed from 15.5 cm onwards (the hexagonal crystals disappear earlier than elongated ones. They are not seen in the subsample 3-5.5 cm from the inlet).

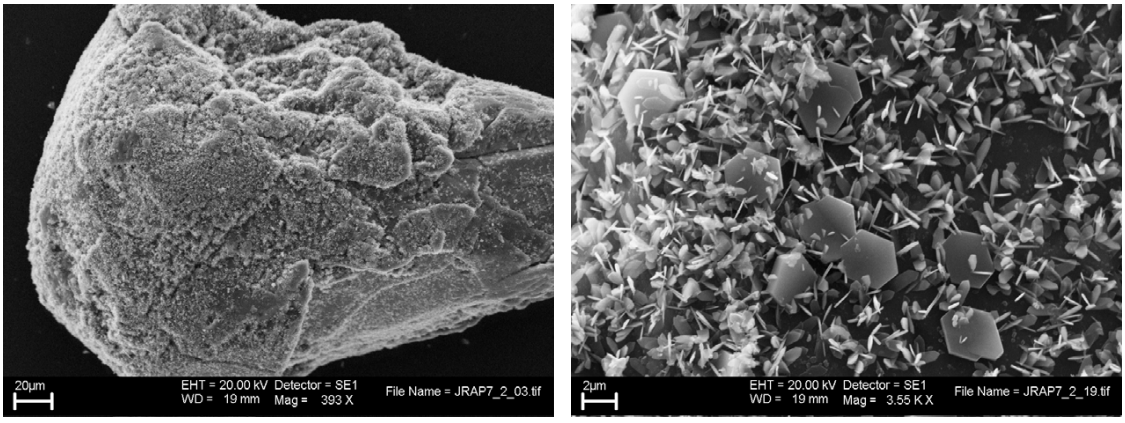

a b

Figure 4 Secondary electron photomicrographs. (a) quartz grain coated with a thin layer of Al-rich crystals (subsample 0-3 cm). (b) elongated and hexagonal crystals of Al-rich phases (subsample 0-3 cm).

In the subsample 15.5-18 cm, a different type of precipitate is present. This phase predominantly comprises of Fe and Ca with minor Ni. It occurs either attached to grains or as discrete crystals scattered in between the grains. It forms aggregates < 10μm in size, of euhedral to subhedral, locally pseudocubical crystals. These aggregates are not associated with any particular phase. The amount of Fe-rich aggregates varies over the interval from 15.5-30.5 cm, but probably never exceeds 1% of the total bulk composition.

An amorphous coating sporadically formed on some labradorite grains, and is composed of Al, Na, Mg, Ca, Fe – silicate?. In addition, a small amount of halite was seen in some samples. This, however, was insignificant.

5. Discussion

The aim of this work was to provide a well-constrained laboratory experiment reacting known quantities of minerals with CO_2-rich fluids, to simulate situations where CO_2 is being injected into lithologies deep underground. The experimental results can also be used as a test case for predictive geochemical computer modelling. Such models will help improve our ability to predict the long-term fate of CO_2 stored underground.

The experiment, though complex in terms of equipment, was successful in that a run time of approximately 3.5 months was achieved together with the recovery of the intact column from the equipment at the end of the experiment. This column was then examined for mineralogical changes and the collected fluids analysed to provide data on the fate of the dissolved species.

Using a specially developed cell it was also possible to obtain a measurement of pH under in-situ conditions (temperature and pressure) which gave an in-situ pH (at 130°C, 300 bar) = 4.7. For most of the experiment, there was little change in the concentration of sodium and chloride concentrations from the starting values. Calcium showed an initial two-fold increase in concentration, which then remained steady for the remainder of the experiment. This increase was likely due to dissolution of the calcite in the mineral assemblage. Magnesium, showed a similar trend to that of calcium. Aluminium and potassium concentrations throughout the experiment were close to or below that of the analytical detection limit.

Analysis of the solid samples from the experiment revealed changes in calcite morphology from the beginning of the experimental column. There was complete removal of calcite from 10 cm to 30 cm into the column, with original calcite only being observed after approximately 30 cm from the column inlet. Labradorite also showed signs of dissolution in the early part of the column, but from 18 cm, onwards it remained mostly fresh with minor corrosion. Other starting mineral phases did not show any significant changes after reaction with the CO_2-rich fluid. There is some limited evidence to suggest that kaolinite and/or an Al hydroxide phase formed in the early part of the column. SEM-EDXA and XRD analysis suggest the formation of secondary calcite cement towards the end of the column.

Acknowledgements

The authors would like to thank their BGS colleagues whose contributions have helped make this report possible. In particular, Humphrey Wallis and Steve Upton of the R&D workshops provided technical assistance and modified the pressure vessels used for the experiments. Helen Taylor, Richard Shaw and Claire Williams performed the chemical analysis. This paper is published with the permission of the Executive Director, British Geological Survey (NERC).

List of references

- [1] Schremp, F.W. and Roberson, G.R. Effect of supercritical carbon dioxide (CO_2) on construction materials. Society of Petroleum Engineers Journal, June 1975:227–233.
- [2] Pearce JM, Czernichowski-Lauriol I., Rochelle CA, Springer N, Brosse E, Sanjuan B, Bateman K and Lanini S. How will reservoir and caprock react with injected CO_2 at Sleipner? Preliminary evidence from experimental investigations. Proceedings of the 5th International Conference on Greenhouse Gas Control Technologies (GHGT-5), Cairns, Queensland, Australia. 2000.
- [3] Bateman K., Turner G., Pearce J.M., Noy D.J., Birchall D., Rochelle C.A. Large-scale column experiment: study of CO_2, porewater, rock reactions and model test case. Oil and Gas Science and Technology – Rev. IFP, 2005;60:161-175.